Journal of Neuroradiology 46 (2019) 130–135

Available online at ScienceDirect www.sciencedirect.com

Elsevier Masson France EM|consulte www.em-consulte.com

Original Article

Clinical equivalence assessment of T2 synthesized pediatric brain magnetic resonance imaging☆

Basile Kerleroux[a], Tobias Kober[b,c,d], Tom Hilbert[b,c,d], Maxence Serru[a], Jean Philippe[a,e], Dominique Sirinelli[a,e], Baptiste Morel[a,e,*]

[a] Department of Pediatric Radiology, Clocheville University Hospital, CHRU de Tours, 49, boulevard Béranger, 37044 Tours, France
[b] Advanced Clinical Imaging Technology, Siemens Healthcare AG, Switzerland
[c] Department of Radiology, University Hospital Lausanne (CHUV), Lausanne, Switzerland
[d] LTS5, École Polytechnique Fédérale de Lausanne (EPFL), Lausanne, Switzerland
[e] Faculty of Medicine, François-Rabelais University, 2, boulevard Tonnellé, 3700 Tours, France

ARTICLE INFO

Article history:
Available online 4 May 2018

Keywords:
Synthesized brain MRI
Pediatric radiology
Quantitative imaging
Simulated contrast

ABSTRACT

Background and purpose. – Automated synthetic magnetic resonance imaging (MRI) provides qualitative, weighted image contrasts as well as quantitative information from one scan and is well-suited for various applications such as analysis of white matter disorders. However, the synthesized contrasts have been poorly evaluated in pediatric applications. The purpose of this study was to compare the image quality of synthetic T2 to conventional turbo spin-echo (TSE) T2 in pediatric brain MRI.
Materials and methods. – This was a mono-center prospective study. Synthetic and conventional MRI acquisitions at 1.5 Tesla were performed for each patient during the same session using a prototype accelerated T2 mapping sequence package ($TA_{synthetic}$ = 3:07 min, $TA_{conventional}$ = 2:33 min). Image sets were blindly and randomly analyzed by pediatric neuroradiologists. Global image quality, morphologic legibility of standard structures and artifacts were assessed using a 4-point Likert scale. Inter-observer kappa agreements were calculated. The capability of the synthesized contrasts and conventional TSE T2 to discern normal and pathologic cases was evaluated.
Results. – Sixty patients were included. The overall diagnostic quality of the synthesized contrasts was non-inferior to conventional imaging scale ($P = 0.06$). There was no significant difference in the legibility of normal and pathological anatomic structures of synthetized and conventional TSE T2 (all $P > 0.05$) as well as for artifacts except for phase encoding ($P = 0.008$). Inter-observer agreement was good to almost perfect (kappa between 0.66 and 1).
Conclusions. – T2 synthesized contrasts, which also provides quantitative T2 information that could be useful, could be suggested as an equivalent technique in pediatric neuro-imaging, compared to conventional TSE T2.

Introduction

Automated synthetic magnetic resonance imaging (SyntMRI) was first experimented by Reiderer et al. [1]. The feasibility of SyntMRI was well studied and contrasts were compared to conventionally acquired images in adult neuroradiology [2–10]. Conversely, in pediatric neuroradiology, the synthesized contrasts were poorly evaluated. Few sample trials experiment with such a technique in a pediatric population were reported in the literature [11,12]. The results of these first pilot studies suggest that the synthesized contrasts may be acceptable for clinical use. Some limitations have been described in both adult and pediatric research but affected mostly FLAIR imaging. The synthesized contrasts would suit especially pediatric neuroradiology especially, because it also provides quantitative information about the T2 relaxation in the whole brain [5]. This information would be very helpful for some major pediatric considerations such as the assessment of white matter myelination and maturation [11,13]. Furthermore, one asset of this technique is to provide additional information without substantial elongation of the acquisition time compared with

☆ This study was performed from May to October 2017, Department of Pediatric Radiology, Clocheville University Hospital, CHRU de Tours, France.

* Corresponding author at: Department of Pediatric Radiology, Clocheville Pediatric University Hospital, CHRU de Tours, 49, boulevard Béranger, 37044 Tours, France.
E-mail address: baptiste.morel@univ-tours.fr (B. Morel).

https://doi.org/10.1016/j.neurad.2018.04.003
0150-9861/

conventional TSE T2 [6,11,12]. The aim of our study was to compare the overall image quality of synthetic T2 to conventional TSE T2 in pediatric brain MRI and to assess morphologic legibility, artifacts and capability of identifying and classifying pathologic cases.

Materials and methods

Population

This is a mono-center prospective case-control study. We obtained approval by the local Ethics Committee in Human research (RNI-2017-0XX). All patients gave their informed consent. Patients under 18 years old were recruited from the pediatric university hospital. All complete cases with synthetic and conventional acquisitions were included.

Acquisition parameters

Synthetic and conventional MRI acquisitions at 1.5 Tesla were performed for each patient during the same session using a prototype accelerated T2 mapping sequence package. The MRI scanner was a 1.5 Tesla device (MAGNETOM Aera, Siemens Healthcare GmbH, Erlangen, Germany). First, conventional images were acquired including a 2D axial T2-weighted TSE acquisition (TA = 2:33 min, TR/TR = 9170/105 ms, in-plane resolution = $0.8 \times 0.6\,mm^2$, FOV = $150 \times 150\,mm^2$, 35 slices, slice thickness = 3 mm, twofold GRAPPA acceleration). Additionally, an undersampled multi-echo spin-echo sequence (GRAPPATINI, Hilbert et al. ISMRM 2014) was performed at the end of the exam used for T2 mapping and subsequent synthesized contrast generation (TA = 3:07, TR = 4880 ms, 16 echoes, ΔTE = 105 ms, in-plane resolution $0.8 \times 0.6\,mm^2$, FOV = $150 \times 150\,mm^2$, 35 slices, slice thickness = 3, fivefold undersampling, two concatenations).

Image reconstruction

A combination of parallel imaging and model-based reconstruction was applied to obtain the quantitative T2 maps and equilibrium magnetization images M0 directly at the scanner (GRAPPATINI, Hilbert et al. ISMRM 2014). The model-based reconstruction uses a mathematical signal model (mono-exponential decay) as prior knowledge in an iterative reconstruction, which allows recovering the missing k-space samples lost due to the undersampling. After the T2 map and the M0 image were obtained, the same mathematical signal model was used to generate synthetic contrasts, also online as part of the scanner image reconstruction. The echo time of the synthetic contrast can be chosen arbitrarily. For comparison to the conventional TSE T2 images, a matched TE = 105 ms was used.

Radiological assessments

For each patient, two anonymized sets of images were extracted by an external technician, one with the Conventional TSE T2 and one with the synthesized T2 contrasts. An independent expert pediatric neuroradiologist (DS) with access to all images and clinical files marked each subject as either normal or pathologic. Each pathologic subject was also categorized into disease subtypes. The individual image sets were blindly analyzed by a pediatric neuroradiologist and a fellow in neuroradiology (BM and BK) on standard *syngo*. via workstations (Siemens Healthcare GmbH, Erlangen, Germany). Reviewing was scheduled in three sessions which included a randomized combination of conventional and synthetic T2 images. The two sets (conventional and synthetic) for the same patient were never reviewed in the same session.

Assessment criteria

To assess the image quality, we created a qualitative score inspired by Tanenbaum et al. [6] and Betts et al. [11]. We evaluated successively:

- the global image quality (GIQ);
- the morphologic legibility of several key structures: supra tentorial white/gray matter differentiation (GM/WM), central sulcus (CS), head of the caudate nucleus (head NC), posterior limb of the internal capsule (post limb IC), cerebral peduncle (Cbral ped), mild cerebellar peduncle (MCbelar ped), cervicomedullary junction (CMJ);
- the artifacts: low signal-to-noise (low S/N), overall motion, aliasing, spike noise, phase encoding, fluid pulsation (cerebrospinal fluid, artery or sigmoid sinus pulsation), blurring;
- the capability to identify pathologic cases. For the overall quality and legibility of the key structures, a Lickert 4-point assessment scale was used: inadequate (0) – sufficient (1) – good (2) – excellent (3). 0–1 was considered as non-acceptable (NA) and 2–3 as acceptable (A) for clinical use. For artifact, another 4-point scale was used: one (0) – mild (1) – moderate (2) – severe (3) grouped for analysis as 0–1 acceptable and 2–3 non-acceptable.

Statistical analysis

Statistical computing was performed with the free software R Ver. 3.2.1 (R Foundation for Statistical Computing, Vienna, Austria. URL). For each item, numerical scales were dichotomized as acceptable or not acceptable for clinical use as described below. The Fisher exact test was used to compare the qualitative results thus obtained. *P*-values < 0.05 were considered statistically significant. Inter-observer kappa agreements were calculated.

Results

Study population

Sixty pediatric patients were included (33 males and 27 females). The average age was 55 months (4 years and 7 months); the median age was 28 months (2 years and 4 months) with a range from 4 months to 205 months.

Image quality assessment

Mean assessment score, qualitative rate distribution and corresponding *P*-value is exposed in Table 1 for global image quality, Table 2 for morphologic legibility and Table 3 for artifacts. Global image quality of the synthesized contrasts was non-inferior to conventional imaging scale ($P = 0.06$) for the two physicians (Table 1). There was no significant difference in the legibility of normal and pathological anatomic structures of synthetic and conventional T2 (all $P > 0.05$) (Table 4) as well as for artifacts except for phase encoding ($P \leq 0.01$) and fluid pulsation artifact ($P < 0.01$) (Tables 2 and 3). The Fig. 1 shows comparable synthetic and conventional case-control images from a normal subject at different levels to expose most of the anatomic structures evaluated.

Inter-observer variability

Inter-observer agreements were good to almost perfect (kappa between 0.66 and 1) as detailed in the Table 5.

Table 1
Mean assessment score, qualitative rate distribution and corresponding *P*-value were exposed for global image quality for synthesized contrasts (Synt) and conventional (Conv). Rates 2–3 were considered as acceptable (A) for clinical use, while rates 0–1 were considered as non-acceptable (NA).

	Observer 1							Observer 2						
	Mean value		Qualitative IQ				*P*	Mean value		Qualitative IQ				*P*
	Synt	Conv	Synt		Conv			Synt	Conv	Synt		Conv		
			NA	A	NA	A				NA	A	NA	A	
Global image quality	2.62	2.98	5	55	1	59	0.06	2.55	2.95	5	55	1	59	0.06

Table 2
Mean assessment score, qualitative rate distribution and corresponding *P*-value is exposed for morphologic legibility of several keys structures: supra tentorial white/gray matter differentiation (GM/WM), central sulcus (CS), head of the caudate nucleus (head NC), posterior limb of the internal capsule (post limb IC), cerebral peduncle (Cbral ped), mild cerebrelar peduncle (MCbelar ped), cervicomedullary junction (CMJ). Rates 2–3 were considered as acceptable (A) for clinical use, while rates 0–1 were considered as non-acceptable (NA).

	Observer 1							Observer 2						
	Mean value		Qualitative rate				*P*	Mean value		Qualitative rate				*P*
	Synt	Conv	Synt		Conv			Synt	Conv	Synt		Conv		
			NA	A	NA	A				NA	A	NA	A	
GM/WM	2.67	2.98	5	55	0	60	0.06	2.77	2.97	3	57	0	60	0.24
CS	2.70	2.97	5	55	0	60	0.06	2.72	2.95	5	55	0	60	0.06
Head NC	2.65	2.93	5	55	0	60	0.06	2.68	2.90	5	55	0	60	0.06
Post limb IC	2.77	3.00	5	55	0	60	0.06	2.78	2.98	5	55	0	60	0.06
Cbral ped	2.73	2.98	5	55	0	60	0.06	2.78	2.97	4	56	0	60	0.12
MCbelar ped	2.75	2.97	5	55	0	60	0.06	2.82	2.95	4	56	0	60	0.12
CMJ	2.68	2.92	5	55	1	59	0.21	2.72	2.90	4	56	1	59	0.20

Table 3
Mean assessment score, qualitative rate distribution and corresponding *P*-value were provided for artifacts: low signal-to-noise (low S/N), overall motion, aliasing, spike noise, phase encoding, fluid pulsation (cerebrospinal fluid, artery or sigmoid sinus pulsation), blurring. Rates 0–1 were considered as acceptable (A) for clinical use, while rates 2–3 were considered as non-acceptable (NA).

	Observer 1							Observer 2						
	Mean value		Qualitative rate				*P*	Mean value		Qualitative rate				*P*
	Synt	Conv	Synt		Conv			Synt	Conv	Synt		Conv		
			NA	A	NA	NA				NA	A	NA	A	
Low S/N	0.25	0.07	0	60	2	58	0.49	0.25	0	0	60	2	58	0.49
Overall motion	0.27	0.03	4	56	1	59	0.36	0.30	0.13	5	55	3	57	0.71
Aliasing	0.03	0.03	0	60	0	60	1.00	0.03	0.03	0	60	0	60	1.00
Spike noise	0	0	0	60	0	60	1.00	0	0	0	60	0	60	1.00
Phase encoding	0.85	0.02	4	56	0	60	0.12	1.05	0.15	1	59	11	49	**0.01**
Fluid pulsation	0.72	0.15	20	40	4	56	**0.01**	0.86	0.14	17	43	4	56	**0.01**
Blurring	0	0	0	60	0	60	1.00	0	0	0	60	0	60	1.00

Table 4
Distribution of pathologic cases.

Pathologic cases ($n = 17$)	
Type	Number of cases
Hydrocephalus/large ventricles	5
Hypoxic ischemic injury	3
Leukodystrophy	2
Malformations of cortical development	2
Low grade glioma	1
Persistent Blake pouch cyst	1
Globus pallidus solitary T2/flair intensity	1
Unclassified cerebellar dysplasia	1
Cerebellar hematoma	1

Diagnostic performance

Forty-three cases were healthy and seventeen were pathologic, including various brain diseases encountered in clinical pediatric practice (Table 4). Figs. 2 and 3 show comparable synthetic and conventional case-control images from various pathologic subjects. Considering the classification by DS (who had access to all images and clinical files) as reference, both observers detected all the 17 pathologic cases.

Discussion

In this prospective randomized study, we compared various standard quality parameters such as global image quality, legibility of well-known anatomic structures and usual artifacts after simplifying the assessment with a demanding dichotomized scale. Considering these parameters, the synthesized T2 contrasts seems to be an overall equivalent to standard TSE T2 for clinical practice in pediatric neuroradiology, after awareness of the rise of some artifacts. This larger validation of the synthesized contrasts in pediatric neuroradiology will enable the development of clinical applications for this special population. We chose a binary scale in order to improve the confidence of this imaging. Indeed, we considered acceptable for clinical use, only rates over or equal to 2 (according a Lickert 4-point scale) while Betts et al. considered all rates over or equal to 1 (opposite for artifacts: A = 0–1 and NA = 2–3). Regarding artifacts, phase encoding is most common in the synthesized contrasts for one of the two observers ($P < 0.01$). Those artifacts

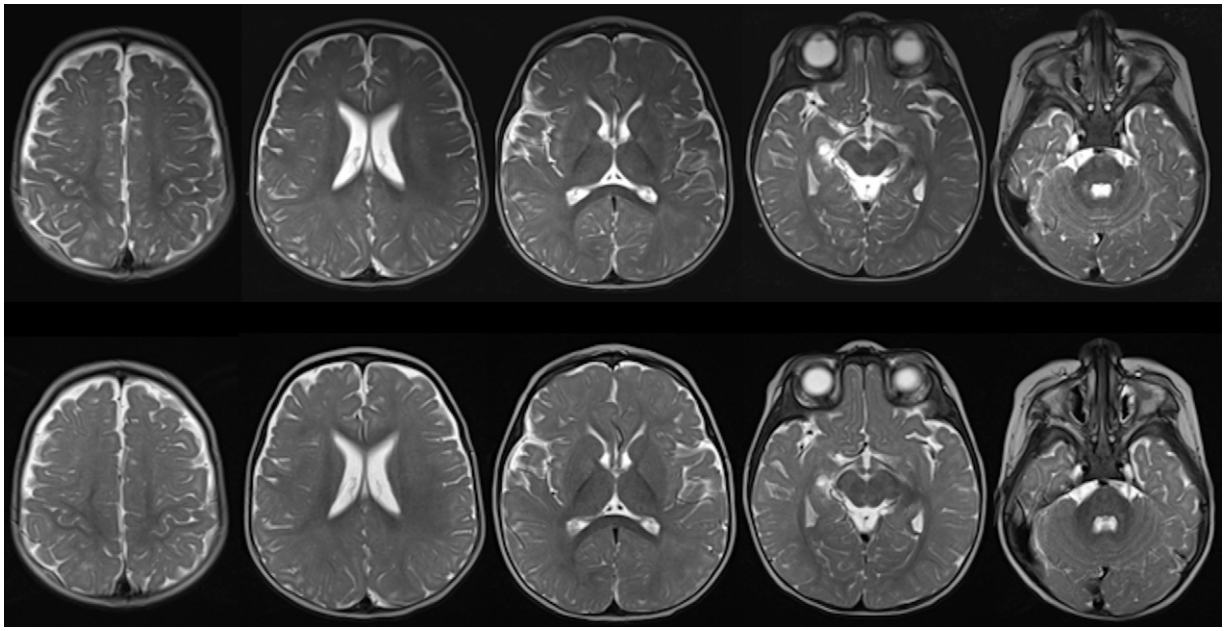

Fig. 1. Axial synthetic (upper row) and conventional (lower row) case-control 1.5 T MR imaging of a normal subject at different relevant levels to exposing most of the anatomic structures evaluated.

Table 5
Inter-observer kappa agreements for each criterion.

KAPPA Obs1 (S)/Obs2 (J)		
	Synt	Conv
Global image quality	0.87	0.84
GM/WM	0.80	0.66
CS	0.97	0.79
Head NC	0.95	0.78
Post limb IC	0.97	1.00
Cbral ped	0.87	0.66
MCbelar ped	0.84	0.79
CMJ	0.86	0.92
Low S/N	0.68	0.66
Overall motion	0.97	1.00
Aliasing	1.00	1.00
Spike noise	1.00	1.00
Phase encoding	0.45	0.14
Fluid pulsation	1.00	1.00
Blurring	1.00	1.00

GM/WM: supra tentorial white/gray matter differentiation; CS: central sulcus; head NC: head of the caudate nucleus; post limb IC: posterior limb of the internal capsule; Cbral ped: cerebral peduncle; MCbelar ped: mild cerebrelar peduncle; CMJ: cervicomedullary junction.

were easily recognizable, very similar from one patient to another and should not be confounded with pathological condition. We also highlighted an increase fluid pulsation artifact. These last artifacts could sometimes disturb the analysis of brain areas such as brain stem or mild cerebellar peduncles. In the presence of these artifacts, additional conventional images should be required, mainly if the underlying pathology or the clinical symptoms suggest potential damage of these structures. This work also demonstrated the feasibility of the synthesized contrasts without crucial elongation of acquisition time ($TA_{synthetic}$ = 3:07 min, $TA_{conventional}$ = 2:33 min). This is an important point in pediatric, especially when MRI is performed without general anesthesia, because motion artifacts are more probable with longer acquisition time [14]. Besides, even for exams under deep sedation, increased anesthesia time may increase the risk of morbidity or complications [15]. There was some limitation in this study. Since all the images were acquired at 1.5 Tesla, an equivalent validation could be required at 3 Tesla. Despite the respect of the rigorous precautions required for a case-control study, at the end of the study, the two neuroradiologists were sometimes able to recognize the conventional from the synthesized one, thanks to their experience of conventional imaging. No conclusion could be reached regarding clinical utility, mainly because the principal objective was not to assess the sensibility and specificity to detect and characterize pathologic condition. The synthesized contrasts could be very promising in pediatric neuroradiology. Indeed, the major benefit of this technique is to provide quantitative information about the inherent tissue relaxation [16] that could be used to build normative databases of healthy subjects, which may be helpful to assess white matter myelination and maturation. With this information, we aim at developing real time personalized sequences considering the tissue features of each developing brain in future. It should be also noted that with the synthetic contrast generation the TE of the T2 weighting may be changed retrospectively after the acquisition and thus also provides PD weighted images without additional acquisition time. Furthermore, adult studies have shown the capability of the synthesized contrasts to measure the modification of tissue relaxation in various brain injuries such as multiple sclerosis [7,17–20]. Similarly, new applications still remain to be discovered in pediatric neuroradiology and may be additional tools for the characterization of brain tumor and inherited or acquired metabolic/toxic disorders. Besides, the knowledge about tissue relaxation may be interesting for the development of automatic segmentation tools, which are able to discern white, grey matter and CSF [13,21–24].

Conclusion

Synthesized T2 contrasts, which also provide quantitative T2 information, could be suggested as an equivalent technique in pediatric neuro-imaging, compared to conventional T2 based on TSE. However, in some cases, the synthesized contrast may suffer from more artifacts. Most of these artifacts were easily recognizable and are most likely not confounded with pathological conditions, but additional conventional images could be required in cases where doubts remain. The synthesized contrasts could be very promising

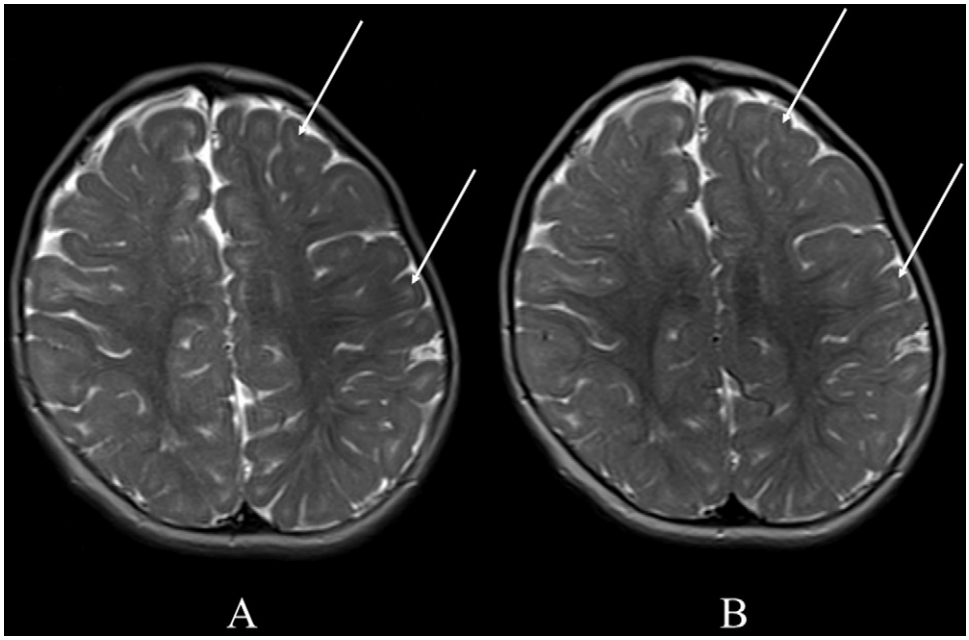

Fig. 2. Axial synthesized (A) and conventional (B) case-control 1.5 T MR imaging of MTHFR inherent deficit with signal abnormality of deep and subcortical U-fiber white matter.

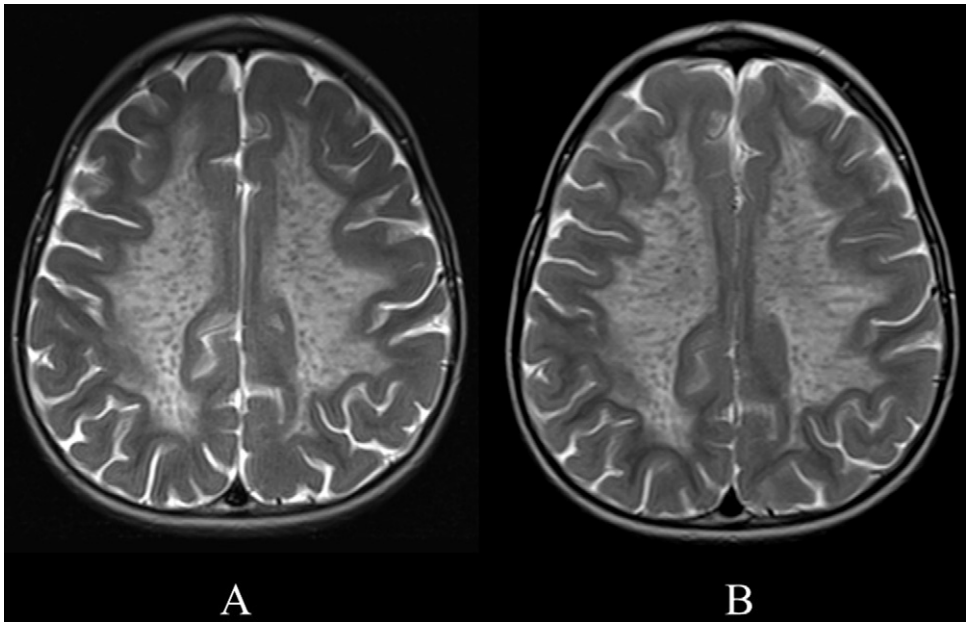

Fig. 3. Axial synthesized (A) and conventional (B) case-control 1.5 T MR imaging of metachromatic leukodystrophy with the characteristic "tigroid" pattern deep white matter signal abnormality.

in pediatric neuroradiology, giving access to new information such as normative databases of tissue relaxation healthy subjects.

Disclosure of interest

The authors declare that they have no competing interest.

References

[1] Riederer SJ, Suddarth SA, Bobman SA, Lee JN, Wang HZ, MacFall JR. Automated MR image synthesis: feasibility studies. Radiology 1984;153:203–6.
[2] Bobman SA, Riederer SJ, Lee JN, Suddarth SA, Wang HZ, MacFall JR. Synthesized MR images: comparison with acquired images. Radiology 1985;155:731–8.
[3] Warntjes JBM, Dahlqvist O, Lundberg P. Novel method for rapid, simultaneous T1, T2*, and proton density quantification. Magn Reson Med 2007;57:528–37.
[4] Warntjes JBM, Leinhard OD, West J, Lundberg P. Rapid magnetic resonance quantification on the brain: optimization for clinical usage. Magn Reson Med 2008;60:320–9.
[5] Krauss W, Gunnarsson M, Andersson T, Thunberg P. Accuracy and reproducibility of a quantitative magnetic resonance imaging method for concurrent measurements of tissue relaxation times and proton density. Magn Reson Imaging 2015;33:584–91.
[6] Tanenbaum LN, Tsiouris AJ, Johnson AN, Naidich TP, DeLano MC, Melhem ER, et al. Synthetic MRI for clinical neuro-imaging: results of the magnetic resonance image compilation (MAGiC) prospective, multicenter, multireader trial. AJNR Am J Neuroradiol 2017.
[7] Deoni SCL. Quantitative relaxometry of the brain. Top Magn Reson Imaging 2010;21:101–13.
[8] Gulani V, Schmitt P, Griswold MA, Webb AG, Jakob PM. Towards a single-sequence neurologic magnetic resonance imaging examination:

multiple-contrast images from an IR TrueFISP experiment. Invest Radiol 2004;39:767–74.
[9] (esr) ES of R. Magnetic Resonance Fingerprinting – a promising new approach to obtain standardized imaging biomarkers from MRI. Insights Imaging 2015;6:163–5.
[10] Ma D, Gulani V, Seiberlich N, Liu K, Sunshine JL, Duerk JL, et al. Magnetic resonance fingerprinting. Nature 2013;495:11971.
[11] Betts AM, Leach JL, Jones BV, Zhang B, Serai S. Brain imaging with synthetic MR in children: clinical quality assessment. Neuroradiology 2016;58:1017–26, http://dx.doi.org/10.1007/s00234-016-1723-9.
[12] West H, Leach JL, Jones BV, Care M, Radhakrishnan R, Merrow AC, et al. Clinical validation of synthetic brain MRI in children: initial experience. Neuroradiology 2017;59:43–50.
[13] Hagiwara A, Warntjes M, Hori M, Andica C, Nakazawa M, Kumamaru KK, et al. SyMRI of the brain: rapid quantification of relaxation rates and proton density, with synthetic MRI, automatic brain segmentation, and myelin measurement. Invest Radiol 2017;52:647–57.
[14] Andre JB, Bresnahan BW, Mossa-Basha M, Hoff MN, Smith CP, Anzai Y, et al. Toward quantifying the prevalence, severity, and cost associated with patient motion during clinical MR examinations. J Am Coll Radiol 2015;12:689–95.
[15] Ing C, Wall MM, DiMaggio CJ, Whitehouse AJO, Hegarty MK, Sun M, et al. Latent class analysis of neurodevelopmental deficit after exposure to anesthesia in early childhood. J Neurosurg Anesthesiol 2017;29:264–73.
[16] Warntjes JBM, Engström M, Tisell A, Lundberg P. Brain characterization using normalized quantitative magnetic resonance imaging. PLOS One 2013;8:e70864.
[17] Larsson HB, Frederiksen J, Kjaer L, Henriksen O, Olesen J. In vivo determination of T1 and T2 in the brain of patients with severe but stable multiple sclerosis. Magn Reson Med 1988;7:43–55.
[18] Hasan KM, Walimuni IS, Abid H, Wolinsky JS, Narayana PA. Multi-modal quantitative MRI investigation of brain tissue neurodegeneration in multiple sclerosis. J Magn Reson Imaging 2012;35:1300–11.
[19] Bonnier G, Roche A, Romascano D, Simioni S, Meskaldji D, Rotzinger D, et al. Advanced MRI unravels the nature of tissue alterations in early multiple sclerosis. Ann Clin Transl Neurol 2014;1:423–32.
[20] Bonnier G, Roche A, Romascano D, Simioni S, Meskaldji DE, Rotzinger D, et al. Multicontrast MRI quantification of focal inflammation and degeneration in multiple sclerosis. BioMed Res Int 2015;2015:569123.
[21] West J, Warntjes JBM, Lundberg P. Novel whole brain segmentation and volume estimation using quantitative MRI. Eur Radiol 2012;22:998–1007.
[22] Ambarki K, Wåhlin A, Birgander R, Eklund A, Malm J. MR imaging of brain volumes: evaluation of a fully automatic software. Am J Neuroradiol 2011;32:408–12.
[23] Ambarki K, Lindqvist T, Wåhlin A, Petterson E, Warntjes MJB, Birgander R, et al. Evaluation of automatic measurement of the intracranial volume based on quantitative MR imaging. Am J Neuroradiol 2012;33:1951–6.
[24] Andica C, Hagiwara A, Hori M, Nakazawa M, Goto M, Koshino S, et al. Automated brain tissue and myelin volumetry based on quantitative MR imaging with various in-plane resolutions. J Neuroradiol 2017.